

**Title**

Distinct carbon sources affect structural and functional maturation of cardiomyocytes derived from human pluripotent stem cells

**Cláudia Correia<sup>1,2</sup>, Alexey Koshkin<sup>1,2</sup>, Patrícia Duarte<sup>1,2</sup>, Dongjian Hu<sup>3,4</sup>, Ana Teixeira<sup>1,2,#</sup>, Ibrahim Domian<sup>3,4</sup>, Margarida Serra<sup>1,2\*</sup>, Paula M. Alves<sup>1,2\*</sup>**

<sup>1</sup>iBET, Instituto de Biologia Experimental e Tecnológica, Oeiras, Portugal; <sup>2</sup>Instituto de Tecnologia Química e Biológica António Xavier, Universidade Nova de Lisboa, Oeiras, Portugal;

<sup>3</sup>Cardiovascular Research Center, Massachusetts General Hospital, Boston, MA 02114, USA;

<sup>4</sup>Harvard Medical School, Boston, MA 02115, USA; Harvard Stem Cell Institute, Cambridge, MA 02138, USA.

<sup>#</sup>Present Address: ETH Zurich, Department of Biosystems Science and Engineering, Mattenstrasse 26, 4058 - Basel, Switzerland

\*Corresponding authors: Paula Marques Alves and Margarida Serra, Animal Cell Technology Unit, iBET, Instituto de Biologia Experimental e Tecnológica and Instituto de Tecnologia Química e Biológica, Apartado 12, 2781-901 Oeiras, Portugal (Phone: +351 21 446 94 31; FAX:+351 21 442 11 61; e-mail: marques@ibet.pt; mserra@itqb.unl.pt); website: <http://tca.itqb.unl.pt>.

## Supporting Information

### Supplemental Figures

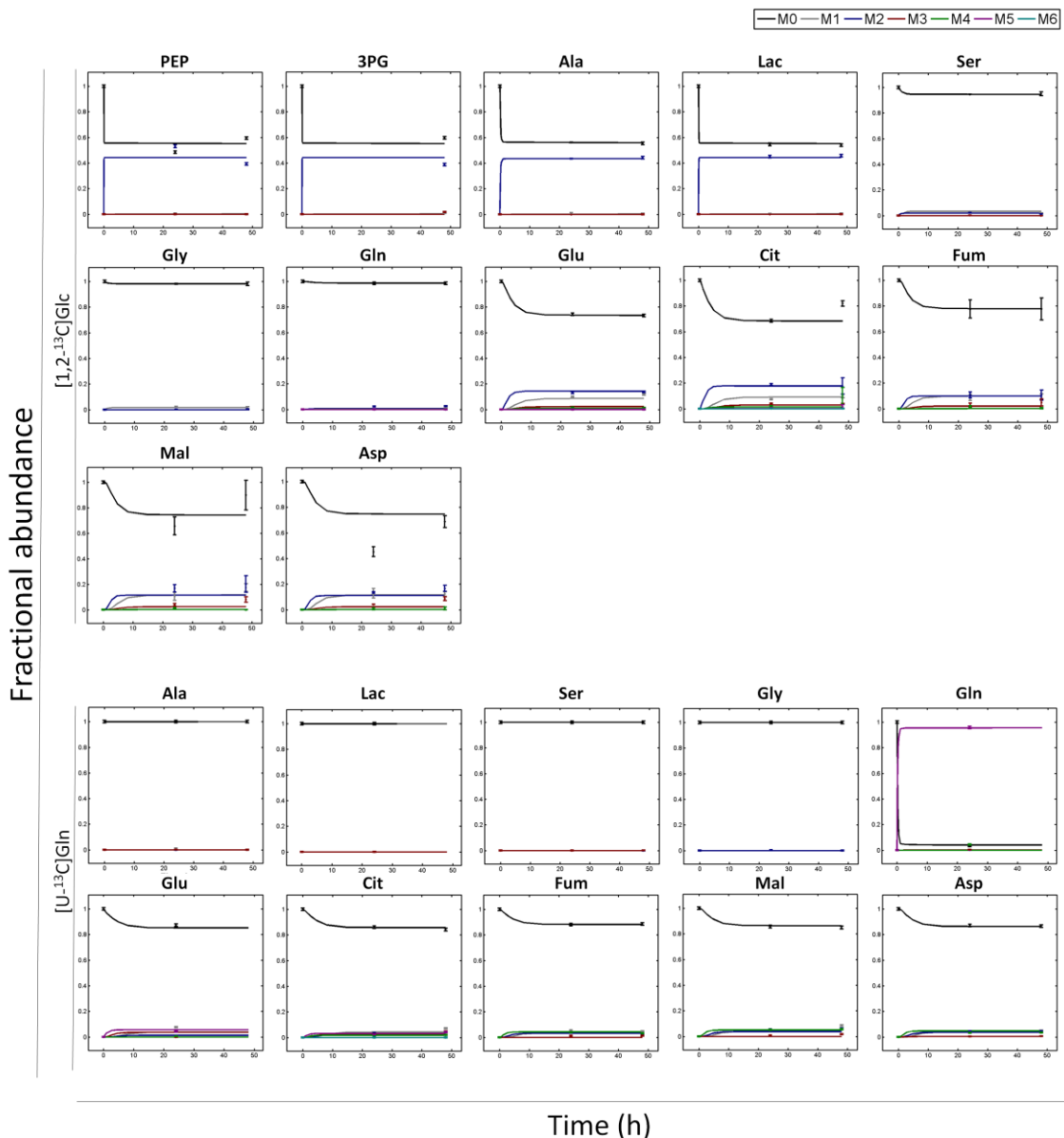


**Fig. S1. Experimental and simulated intracellular  $^{13}\text{C}$ -labelling dynamics in GLCM condition using  $[1,2\text{-}^{13}\text{C}]Glc$  and  $[U\text{-}^{13}\text{C}]Gln$ .** Circle markers correspond to GC-MS measurements corrected for natural isotope abundance. Lines correspond to fitted MIDs from nonstationary  $^{13}\text{C}$ -MFA flux estimation of parallel labelling experiments.

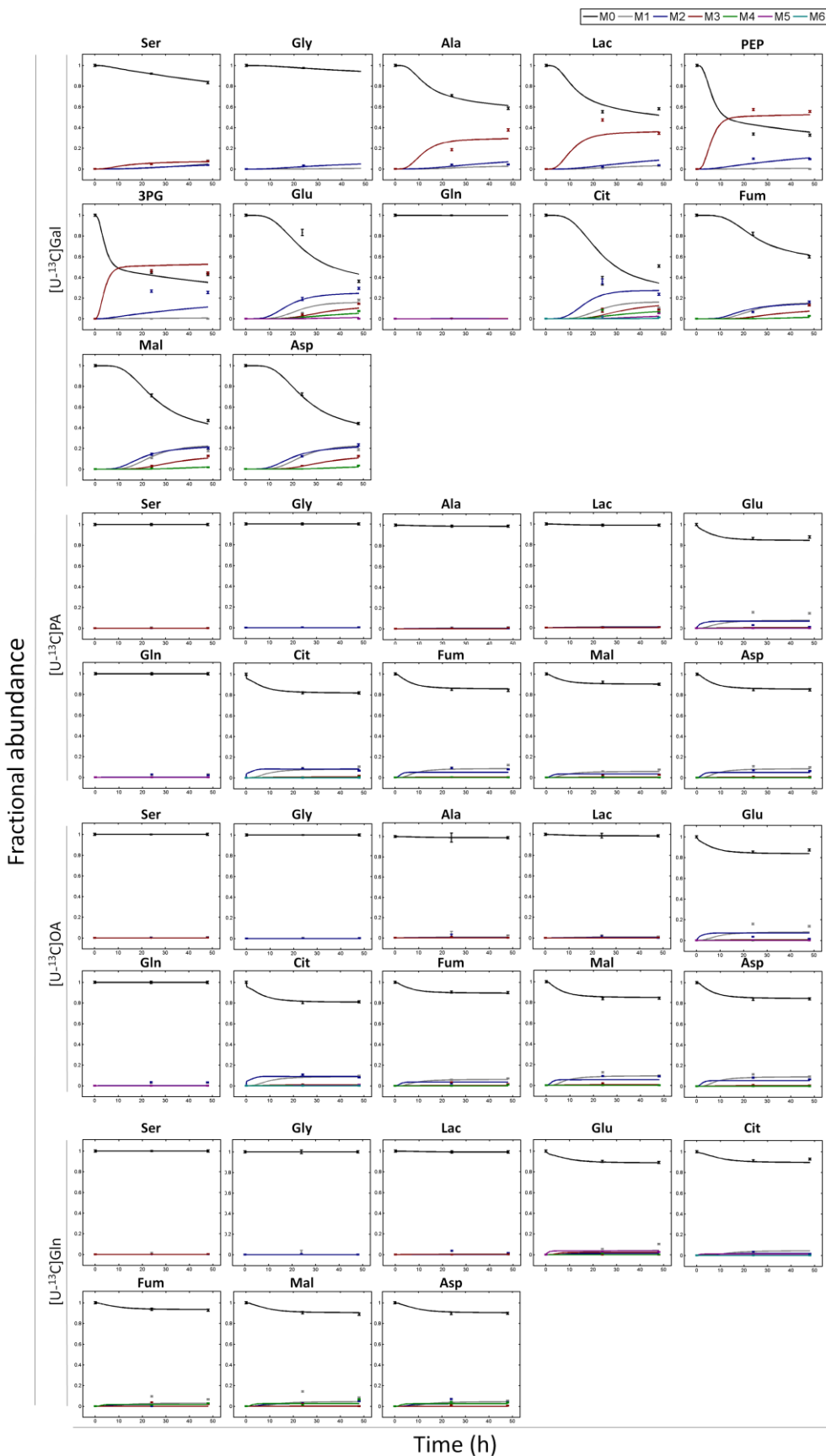


**Fig. S2. Experimental and simulated intracellular  $^{13}\text{C}$ -labelling dynamics in GFAM condition using  $[\text{U}-^{13}\text{C}] \text{GAL}$ ,  $[\text{U}-^{13}\text{C}] \text{PA}$ ,  $[\text{U}-^{13}\text{C}] \text{OA}$  and  $[\text{U}-^{13}\text{C}] \text{Gln}$ . Circle markers correspond to GC-MS**

measurements corrected for natural isotope abundance. Lines correspond to fitted MIDs from nonstationary  $^{13}\text{C}$ -MFA flux estimation of parallel labelling experiments.

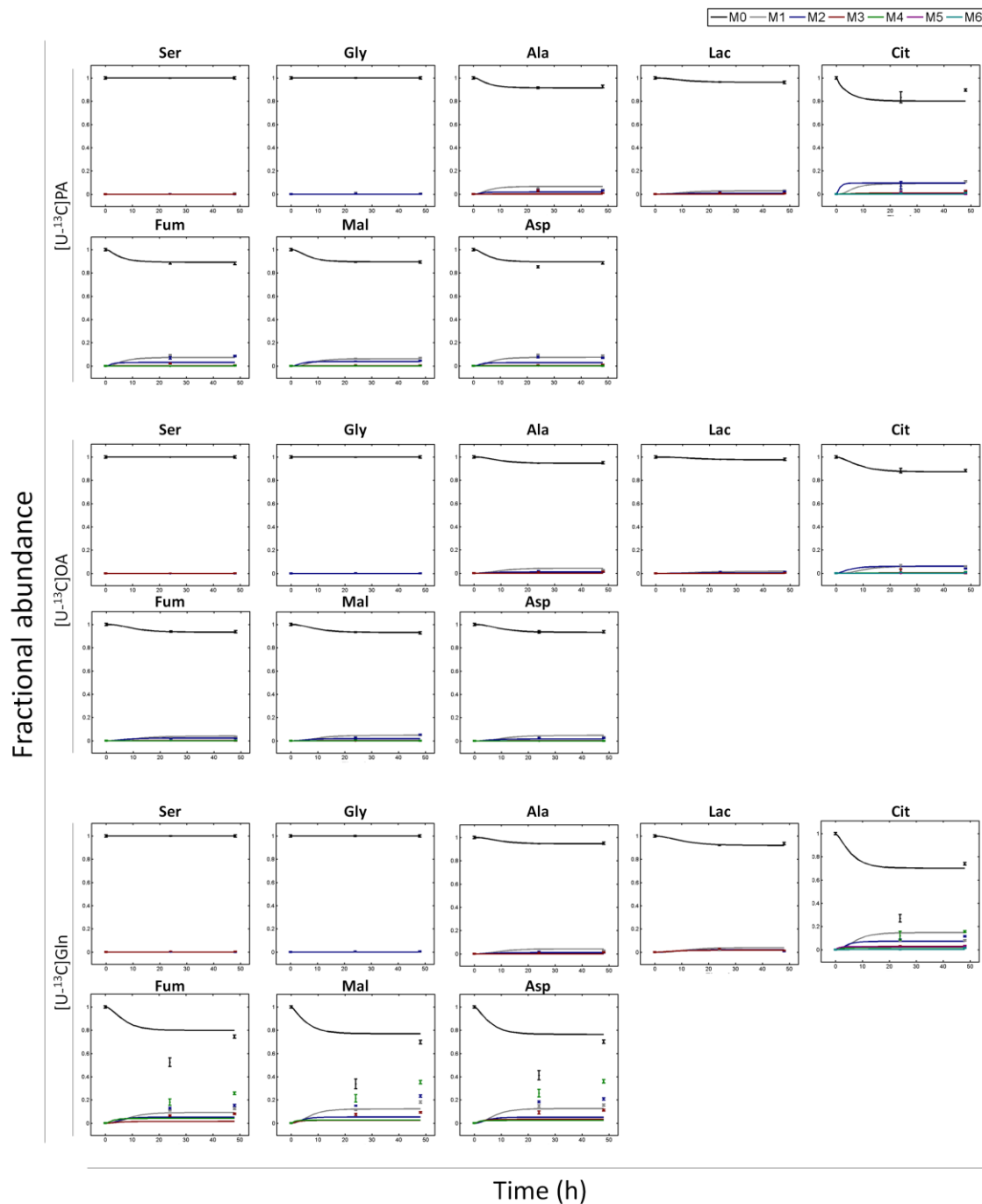


**Fig. S3. Experimental and simulated intracellular  $^{13}\text{C}$ -labelling dynamics in FAM condition using  $[\text{U-}^{13}\text{C}]$ PA,  $[\text{U-}^{13}\text{C}]$ OA and  $[\text{U-}^{13}\text{C}]$ Gln.** Circle markers correspond to GC-MS measurements corrected for natural isotope abundance. Lines correspond to fitted MIDs from nonstationary  $^{13}\text{C}$ -MFA flux estimation of parallel labelling experiments.

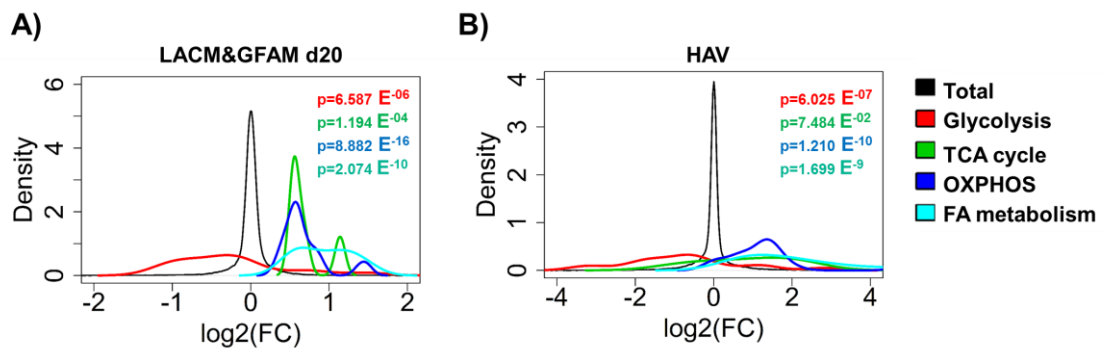


**Fig. S4. Density Plots using R generated with fold change expression of genes from representative metabolic categories for LACM&GFAM d20 (A) and HAV (B).** X axis indicates log<sub>2</sub> fold change in gene expression. Black line indicates expression of all genes. Coloured lines toward the left and right side of the black line indicate down-regulation and up-regulation of pathways, respectively.

# GLCM d20

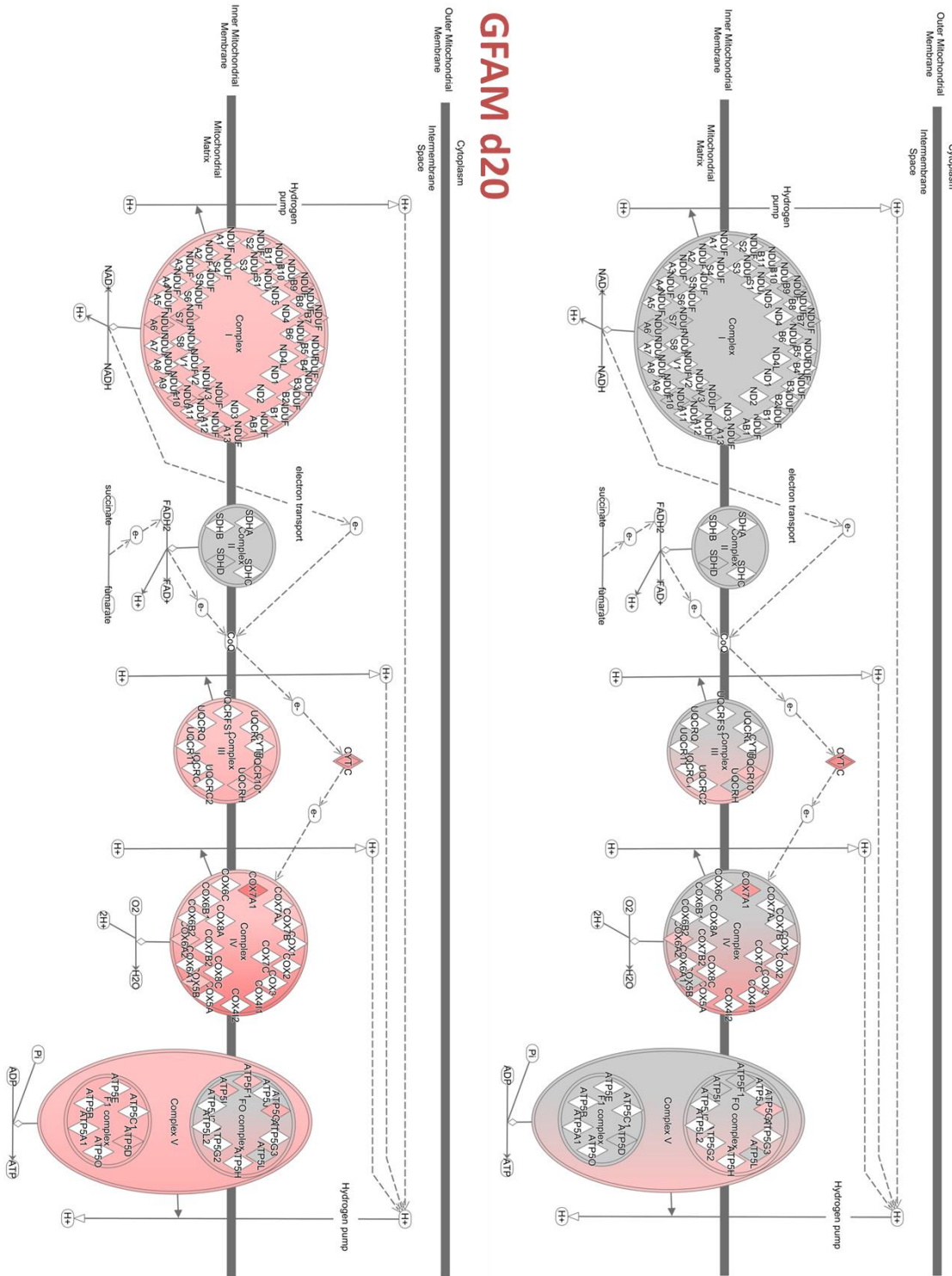


**Fig. S5. Schematic representation of the expression levels of OXPHOS related genes provided by IPA for GLCM and GFAM cultures at day 20. Up-regulated genes are highlighted in red.**

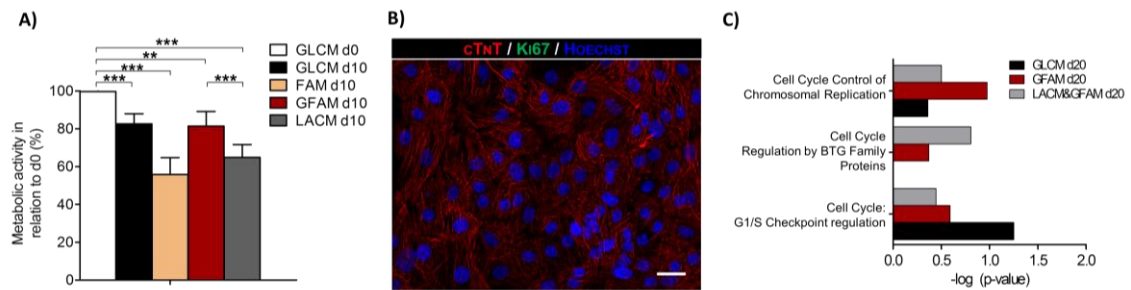


**Fig. S6. Impact of culture media composition on metabolic activity and proliferative capacity.**

(A) Metabolic activity at day 0 and day 10 in all conditions was assessed with PrestoBlue. (B) Representative image of hPSC-CM immunostained for cardiac troponin-T (cTnT) revealing the absence of Ki67<sup>+</sup> cells (green). Nuclei (blue) were stained with Hoechst 33342. Scale bars=30 µm. (C) Adjusted P-value determined by IPA reflecting non-statistically significant enrichment of cell-cycle related pathways in all culture condition.

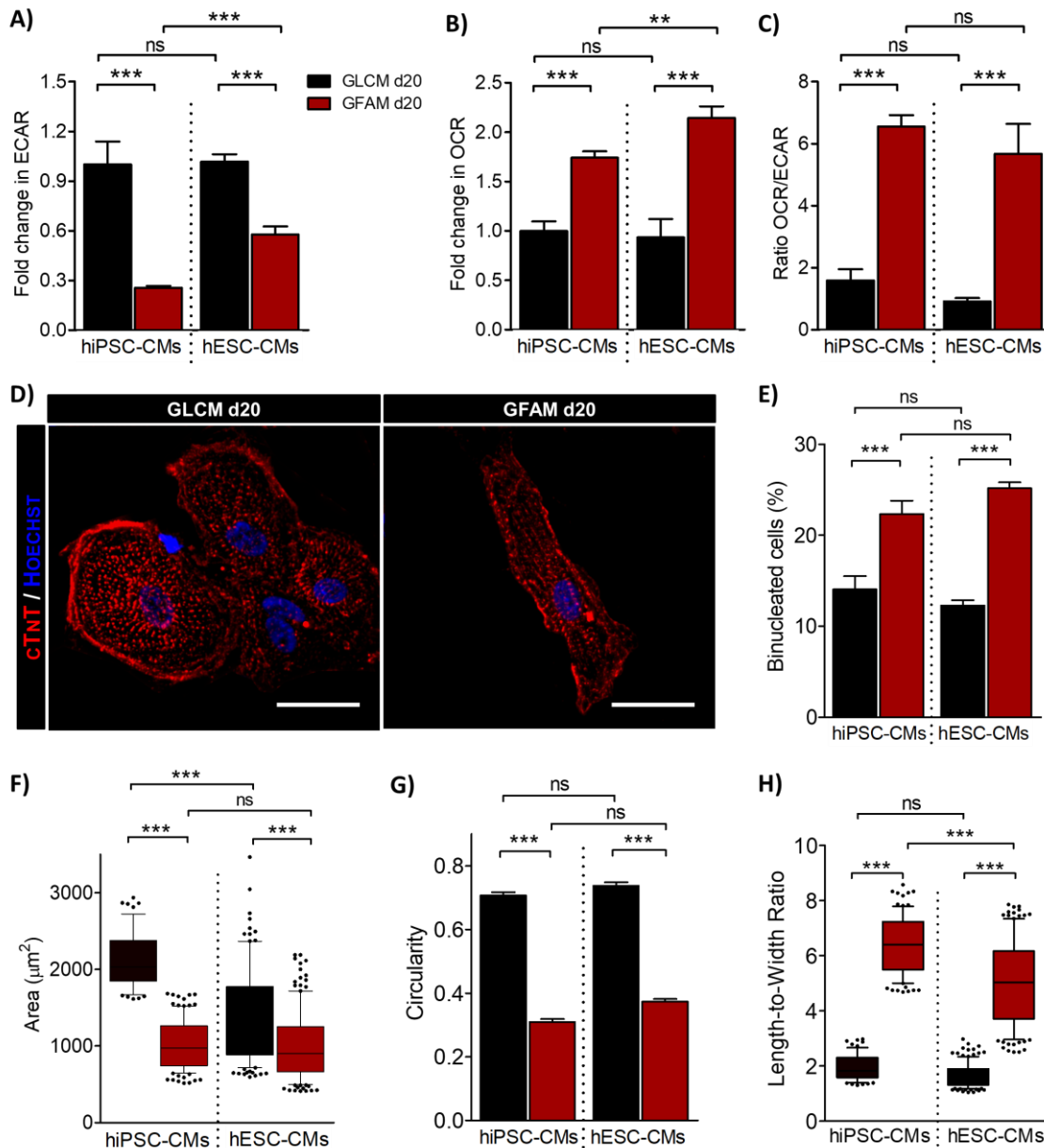


**Fig. S7. Impact of GFAM treatment on hESC-CM metabolism and structure.** hESC-CMs maintained in GLCM and GFAM for 20 days were compared in terms of cellular metabolism and structure between each other and with hiPSC-CMs cultured also in GLCM and GFAM. (A) Extracellular acidification rate (ECAR). (B) Basal oxygen consumption rate (OCR). (C) OCR/ECAR ratio reflecting the relative contribution of OXPHOS over glycolysis for energy generation. (n>20 per condition of 3 different cell batches). (D) Representative images of hPSC-CM immunostained for cardiac troponin-T (cTnT, red). Nuclei (blue) were stained with Hoechst 33342. Scale bars=30  $\mu\text{m}$ . (E) Percentage of binucleated hiPSC-CMs in GLCM and GFAM (n>20 per condition). (F-H) Cell structure characterization in terms of cell area (F), circularity index (G), length-to-width ratio (H). n>70 cells per condition of 3 separate experiments. Data are represented as mean $\pm$ SD.

\* $p<0.05$ ; \*\* $p<0.01$ ; \*\*\* $p<0.001$ ; ns, not significant.

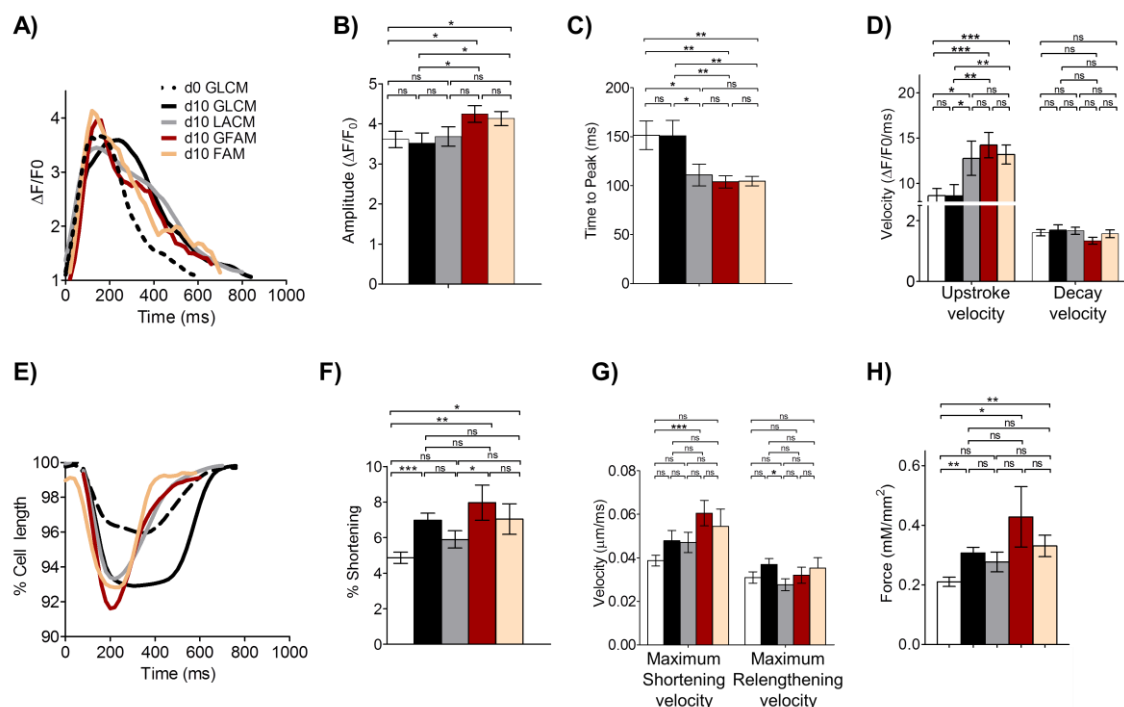


**Fig. S8. Impact of metabolic manipulation in hiPSC-CM functionality.** hiPSC-CMs were analyzed in terms of calcium signaling profiles (A-D) and contractile performance (E-H), before (white) and after 10 days of culture in different culture medium (GLCM-black, LACM -grey, GFAM-red and FAM). Calcium transient kinetic was evaluated by loading the hiPSC-CMs with the intracellular calcium indicator Fluo-4 AM: (A) Representative calcium transients.  $F/F_0$ : change of fluorescence signal over background fluorescence; (B) Calcium transient amplitude ( $F/F_0$ ); (C) Time to peak. (D) Average upstroke and decay velocities.  $n = 24\text{-}35$  cells per condition of 3 separate experiments. Contractile kinetics for each culture condition is described in: (E) Representative contraction curves for each culture condition, reflecting changes in the percentage of cell length. (F) Percentage of shortening; (G) Average shortening and relengthening velocities.  $n = 15\text{-}22$  cells per condition of 3 separate experiments. (H) Maximum contractile force generated.  $n = 8\text{-}17$  cells per condition of 3 separate experiments. Data are represented as mean $\pm$ SEM. \* $p<0.05$ ; \*\* $p<0.01$ ; \*\*\* $p<0.001$ ; ns, not significant.

**Table S1. Metabolic network reactions and simulated fluxes determined by nonstationary  $^{13}\text{C}$ -MFA.** Flux values are shown in units of nmol/( $10^6$ cell.h). Negative flux values indicate that net direction is reverse to the direction indicated. The lower bound (LB) and upper bound (UB) of the 95% confidence intervals determined for each flux are also displayed.

	Equation	GLCM d20			FAM d10			GFAM d20		
		Value	LB	UB	Value	LB	UB	Value	LB	UB
v1	G6P <-> F6P	220.5	[ 150 ; 347.1 ]		0	[ 0 ; 0 ]		3.9	[ 1.8 ; 5.4 ]	
v2	F6P -> FBP	242.9	[ 165 ; 326.2 ]		0	[ 0 ; 0 ]		21.6	[ 15.9 ; 22.3 ]	
v3	FBP <-> DHAP + GAP	242.9	[ 165 ; 326.2 ]		0	[ 0 ; 0 ]		21.6	[ 15.9 ; 22.3 ]	
v4	DHAP <-> GAP	242.9	[ 165 ; 326.2 ]		0	[ 0 ; 0 ]		21.6	[ 15.9 ; 22.3 ]	
v5	GAP <-> 3PG	497.1	[ 338.4 ; 660.4 ]		0	[ 0 ; 0 ]		52	[ 38.1 ; 54 ]	
v6	3PG <-> PEP	496.9	[ 334.3 ; 658.4 ]		0	[ 0 ; 0 ]		49.7	[ 36.8 ; 53.2 ]	
v7	PEP -> Pyr.c	496.9	[ 334.3 ; 658.4 ]		0	[ 0 ; 0 ]		49.7	[ 36.8 ; 53.2 ]	
v8	Pyr.c <-> Pyr.m	5.6	[ 1.4 ; 8.6 ]		109.2	[ 106.3 ; 109.3 ]		72.4	[ 56.3 ; 75.6 ]	
v9	G6P -> P5P + CO2	33.7	[ 0 ; 50.2 ]		0	[ 0 ; 0 ]		26.5	[ 18.8 ; 29.2 ]	
v10	P5P + P5P <-> GAP + S7P	11.2	[ 0 ; 16.7 ]		0	[ 0 ; 0 ]		8.8	[ 6.3 ; 9.7 ]	
v11	S7P + GAP <-> E4P + F6P	11.2	[ 0 ; 16.7 ]		0	[ 0 ; 0 ]		8.8	[ 6.3 ; 9.7 ]	
v12	E4P + P5P <-> GAP + F6P	11.2	[ 0 ; 16.7 ]		0	[ 0 ; 0 ]		8.8	[ 6.3 ; 9.7 ]	
v13	Pyr.c <-> Lac	491.4	[ 336.4 ; 651.4 ]		0	[ 0 ; 0 ]		0	[ 0 ; 0 ]	
v14	Pyr.c <-> Ala	0	[ -7.8 ; 14 ]		0	[ 0 ; 0 ]		-11	[ -12.3 ; -9.1 ]	
v15	Pyr.m -> AcCoA.m + CO2	5.6	[ 2.6 ; 8.6 ]		30.3	[ 30.2 ; 30.3 ]		72.4	[ 54.8 ; 75.3 ]	
v16	OAA.m + AcCoA.m -> Cit.m	14.1	[ 6.3 ; 21.6 ]		55.4	[ 55.3 ; 55.4 ]		88.5	[ 66.5 ; 92.2 ]	
v17	Cit.m <-> AKG + CO2	14.1	[ 6.4 ; 20.3 ]		22.1	[ 22.1 ; 22.2 ]		88.5	[ 66.7 ; 92.1 ]	
v18	AKG -> SucCoA + CO2	14.7	[ 6.9 ; 27.2 ]		43.3	[ 43.2 ; 43.4 ]		95.7	[ 71.1 ; 100.1 ]	
v19	SucCoA <-> Suc	14.7	[ 6.9 ; 27.2 ]		43.3	[ 43.2 ; 43.4 ]		95.7	[ 71.1 ; 100.1 ]	
v20	Suc <-> Fum.m	14.7	[ 6.8 ; 26.7 ]		45.7	[ 45.6 ; 45.9 ]		95.7	[ 72 ; 99.4 ]	
v21	Fum.m <-> Mal.m	14.7	[ 4 ; 22.8 ]		52.1	[ 52.0 ; 52.2 ]		95.7	[ 72.2 ; 99.3 ]	
v22	Mal.m <-> OAA.m	14.1	[ 6.3 ; 21.4 ]		-23.5	[ -23.7 ; -23.4 ]		88.5	[ 66.4 ; 91.5 ]	
v23	Mal.c -> Pyr.c + CO2	0	[ 0 ; 4.2 ]		108.9	[ 108.7 ; 109.5 ]		7.2	[ 4.7 ; 8.3 ]	
v24	Pyr.m + CO2 -> OAA.m	0	[ 0 ; 0 ]		78.9	[ 78.4 ; 79.4 ]		0	[ 0 ; 0.5 ]	
v25	Gln <-> Glu	1	[ 0.4 ; 1.7 ]		3.8	[ 3.6 ; 3.9 ]		2.6	[ 1.9 ; 2.7 ]	

v26	AKG <-> Glu	-0.6	[ -6.4 ; -0.3 ]	-21.2	[ -22.8 ; -20.2 ]	-7.2	[ -8.4 ; -4.8 ]
v27	Asn <-> Asp	0	[ 0 ; 0 ]	0	[ 0 ; 0 ]	0	[ 0 ; 0 ]
v28	3PG -> Ser	0.2	[ 0 ; 13.2 ]	0	[ 0 ; 0 ]	2.3	[ 0.7 ; 3.8 ]
v29	Ser -> Pyr.c	0	[ 0 ; 8.3 ]	0.3	[ 0.2 ; 0.3 ]	4.5	[ 1.1 ; 7 ]
v30	Ser <-> Gly + C1	-1.8	[ -4.1 ; 0 ]	-2.4	[ -2.4 ; -2.4 ]	-0.3	[ -2 ; 0 ]
v31	Glu <-> Pro	0	[ -4.4 ; 3.5 ]	-10.5	[ -10.5 ; -10.5 ]	-1.4	[ -4.1 ; 1.4 ]
v32	Val + CO2 -> Suc + CO2 + CO2	0	[ 0 ; 0.1 ]	0	[ 0 ; 0 ]	0	[ 0 ; 0.5 ]
v33	Ile + CO2 -> Suc + AcCoA.m + CO2	0	[ 0 ; 0.1 ]	0	[ 0 ; 0 ]	0	[ 0 ; 0.5 ]
v34	Leu + CO2 -> AcCoA.m + AcCoA.m + AcCoA.m + CO2	2.2	[ 1.2 ; 3.3 ]	0	[ 0 ; 0 ]	1.6	[ 0.1 ; 2.6 ]
v35	Thr -> AcCoA.m + Gly	0	[ 0 ; 1.6 ]	3.9	[ 3.9 ; 4.0 ]	0.3	[ 0.1 ; 0.6 ]
v36	Phe -> Tyr	0	[ 0 ; 0.1 ]	0	[ 0 ; 0 ]	0	[ 0 ; 0.4 ]
v37	Tyr -> Fum.m + AcCoA.m + AcCoA.m + CO2	0	[ 0 ; 0.1 ]	6.4	[ 6.3 ; 6.4 ]	0	[ 0 ; 0.4 ]
v38	Met + Ser + CO2 -> Suc + Cys.snk + CO2 + C1	0	[ 0 ; 0 ]	2.4	[ 2.4 ; 2.5 ]	0	[ 0 ; 0.4 ]
v39	Lys -> CO2 + CO2 + AcCoA.m + AcCoA.m	0.9	[ 0 ; 1.8 ]	0	[ 0 ; 0 ]	0	[ 0 ; 1.5 ]
v40	His -> Glu + C1	1.8	[ 0 ; 4.2 ]	0	[ 0 ; 0 ]	0.3	[ 0 ; 2 ]
v41	Arg -> Glu + Urea.snk	59.8	[ 0 ; Inf ]	0	[ 0 ; 0 ]	3.6	[ 0 ; 4.1 ]
v42	Glu + CO2 -> Arg	64	[ 0.7 ; Inf ]	0	[ 0 ; 0 ]	2.7	[ 0 ; 2.9 ]
v43	Glc.ext -> G6P	254.2	[ 178 ; 326.1 ]	0	[ 0 ; 0 ]	0	[ 0 ; 0.2 ]
v44	Lac.ext <-> Lac	-491.4	[ -651.4 ; -336.4 ]	0	[ 0 ; 0 ]	0	[ 0 ; 0 ]
v45	Ala.ext <-> Ala	0	[ -14 ; 7.8 ]	0	[ 0 ; 0 ]	11	[ 9.1 ; 12.3 ]
v46	Gln.ext -> Gln	1	[ 0.4 ; 1.7 ]	3.8	[ 3.8 ; 3.8 ]	2.6	[ 1.9 ; 2.7 ]
v47	Glu.ext <-> Glu	2	[ -1.2 ; 5.8 ]	6.9	[ 6.9 ; 6.9 ]	2.1	[ -0.2 ; 4.4 ]
v48	Ser.ext <-> Ser	-1.9	[ -9.7 ; 0.8 ]	0.3	[ 0.2 ; 0.4 ]	1.9	[ 0.7 ; 3.0 ]
v49	Gly.ext <-> Gly	1.8	[ -1.6 ; 4.1 ]	-1.5	[ -1.6 ; -1.4 ]	-0.1	[ -0.6 ; 1.6 ]
v50	Pro.ext <-> Pro	0	[ -3.5 ; 4.4 ]	10.5	[ 10.5 ; 10.5 ]	1.4	[ -1.4 ; 4.1 ]
v51	Val.ext -> Val	0	[ 0 ; 0.1 ]	0	[ 0 ; 0 ]	0	[ 0 ; 0.5 ]
v52	Ile.ext -> Ile	0	[ 0 ; 0.1 ]	0	[ 0 ; 0 ]	0	[ 0 ; 0.5 ]
v53	Leu.ext -> Leu	2.2	[ 1.2 ; 3.3 ]	0	[ 0 ; 0 ]	1.6	[ 0.1 ; 2.6 ]
v54	Thr.ext -> Thr	0	[ 0 ; 1.6 ]	3.9	[ 3.9 ; 4 ]	0.3	[ 0.1 ; 0.6 ]
v55	Phe.ext -> Phe	0	[ 0 ; 0.1 ]	0	[ 0 ; 0 ]	0	[ 0 ; 0.4 ]

v56	Tyr.ext -> Tyr	0	[ 0 ; 0.1 ]	6.4	[ 6.3 ; 6.4 ]	0	[ 0 ; 0.3 ]
v57	Met.ext -> Met	0	[ 0 ; 0 ]	2.4	[ 2.4 ; 2.5 ]	0	[ 0 ; 0.4 ]
v58	Lys.ext -> Lys	0.9	[ 0 ; 1.8 ]	0	[ 0 ; 0 ]	0	[ 0 ; 1.5 ]
v59	His.ext -> His	1.8	[ 0 ; 4.2 ]	0	[ 0 ; 0 ]	0.3	[ 0 ; 2 ]
v60	Arg.ext <-> Arg	-4.2	[ -7 ; -1.3 ]	0	[ 0 ; 0 ]	0.9	[ -2.4 ; 3.8 ]
v61	Asp <-> OAA.c	-0.6	[ -1.8 ; -0.3 ]	0	[ 0 ; 0 ]	0	[ -1 ; 0 ]
v62	Cit.c -> OAA.c + AcCoA.c	0	[ 0 ; 0.1 ]	33.3	[ 33.2 ; 33.3 ]	0	[ 0 ; 1.8 ]
v63	CO2.ext <-> CO2	-5.9	[ -90 ; Inf ]	-132.1	[ -132.2 ; -132.1 ]	-287.8	[ -303.4 ; -213.4 ]
v64	AcCoA.c -> FA.ext	0	[ 0 ; 0.1 ]	33.3	[ 33.2 ; 33.3 ]	0	[ 0 ; 1.8 ]
v65	AP.ext -> AP.c	0	[ 0 ; 0 ]	1.9	[ 1.9 ; 1.9 ]	0.7	[ 0.5 ; 0.7 ]
v66	AP.m -> 8 x AcCoA.m	0	[ 0 ; 0 ]	8x0.6	[ 8x0.6 ; 8x0.7 ]	8x0.7	[ 8x0.5 ; 8x0.7 ]
v67	AO.ext -> AO.c	0	[ 0 ; 0 ]	1.7	[ 1.7 ; 2.3 ]	0.6	[ 0.5 ; 0.7 ]
v68	AO.m -> 9 x AcCoA.m	0	[ 0 ; 0 ]	9x0.4	[ 9x0.4 ; 9x1.5 ]	9x0.6	[ 9x0.5 ; 9x0.6 ]
v69	Gal.ext -> G6P	0	[ 0 ; 0 ]	0	[ 0 ; 0 ]	30.4	[ 22 ; 32.1 ]
v70	Cit.c -> Cit.snk	0	[ 0 ; 1.9 ]	0	[ 0 ; 0 ]	0	[ 0 ; 1.5 ]
v71	Mal.m <-> Mal.c	0.6	[ 0.2 ; 4.4 ]	75.6	[ 75.3 ; 75.7 ]	7.2	[ 4.5 ; 8.3 ]
v72	0*Mal.c -> Mal.s	3.9	[ 0 ; 100 ]	0	[ 0 ; 6.4 ]	0.5	[ 0 ; 100 ]
v73	0*Mal.m -> Mal.s	96.1	[ 0 ; 100 ]	100	[ 93.6 ; 100 ]	99.5	[ 0 ; 100 ]
v74	Mal.s -> Sink	100	[ 100 ; 100 ]	100	[ 100 ; 100 ]	100	[ 100 ; 100 ]
v75	0*Fum.c -> Fum.s	14	[ 6.2 ; 21.6 ]	0	[ 0 ; 0.2 ]	32.2	[ 28.9 ; 36.3 ]
v76	0*Fum.m -> Fum.s	86	[ 78.4 ; 93.8 ]	100	[ 99.8 ; 100 ]	67.8	[ 63.7 ; 71.1 ]
v77	Fum.s -> Sink	100	[ 100 ; 100 ]	100	[ 100 ; 100 ]	100	[ 100 ; 100 ]
v78	Mal.c <-> Fum.c	0	[ 0 ; 0 ]	0	[ 0 ; 0 ]	0	[ 0 ; 0 ]
v79	OAA.c <-> Mal.c	-0.6	[ -1.9 ; -0.2 ]	33.3	[ 33.3 ; 33.3 ]	0	[ -1 ; 0 ]
v80	Asp.ext <-> Asp	-0.6	[ -1.8 ; -0.3 ]	0	[ 0 ; 0 ]	0	[ -1 ; 0 ]
v81	0*Cit.c -> Cit.s	0	[ 0 ; 100 ]	0	[ 0 ; 100 ]	83.5	[ 0 ; 100 ]
v82	0*Cit.m -> Cit.s	100	[ 0 ; 100 ]	100	[ 0 ; 100 ]	16.5	[ 0 ; 100 ]
v83	Cit.s -> Sink	100	[ 100 ; 100 ]	100	[ 100 ; 100 ]	100	[ 100 ; 100 ]
v84	Cit.c <-> Cit.m	0	[ -2 ; 0 ]	-33.3	[ -33.3 ; -33.2 ]	0	[ -1.6 ; 0 ]
v85	AP.c -> AP.m	0	[ 0 ; 0 ]	0.6	[ 0.6 ; 0.7 ]	0.7	[ 0.5 ; 0.7 ]

v86	AP.c -> AP.snk	0 [ 0 ; 0 ]	0.4 [ 0.4 ; 1.5 ]	0.6 [ 0.5 ; 0.6 ]
v87	AO.c -> AO.m	0 [ 0 ; 0 ]	1.3 [ 1.2 ; 1.3 ]	0 [ 0 ; 0.1 ]
v88	AO.c -> AO.snk	0 [ 0 ; 0 ]	1.3 [ 1.3 ; 3.5 ]	0 [ 0 ; 0.1 ]

Abbreviations: G6P. glucose-6-phosphate; F6P. fructose-6-phosphate; FBP. fructose-1,6-bisphosphate; DHAP. Dihydroxyacetone phosphate; GAP. glyceraldehyde 3-phosphate; 3PG. 3-Phosphoglyceric acid; PEP. phosphoenolpyruvate; Pyr. pyruvate; P5P. pentose-5-phosphate; CO2. carbon dioxide; S7P. sedoheptulose-7-phosphate; E4P. erythrose 4-phosphate; Lac. lactate; Ala. alanine; AcCoA. acetyl-CoA; OAA. oxaloacetate; Cit. citrate;  $\alpha$ KG.  $\alpha$ -ketoglutarate; Suc. succinate; Fum. fumarate; Mal. malate; Glu. glutamate; Pro. proline; Val. valine; Ile. isoleucine; Leu. leucine; Thr. threonine; Phe. phenylalanine; Tyr. tyrosine; Met. methionine; Ser. serine; Cys. cysteine; Lys. lysine; His. histidine; Arg. arginine; Gln. glutamine; Asp. aspartate; FA. fatty acid; PA. palmitic acid; AO. oleic acid; c. cytosolic; m. mitochondrial; s. sink.

Fumarate and succinate were considered as symmetric molecules during flux estimation. Compartmentalization of Pyr, Fum, Mal, Cit, AcCoA, OAA, AO and AP pools were taken in account in the model. Sink pools were considered for metabolites that could not be balanced.

Balanced metabolite pools: G6P, F6P, FBP, DHAP, GAP, 3PG, PEP, Pyr.c, Pyr.m, P5P, CO2, S7P, E4P, Lac, Ala, AO.c, AO.m, AP.c, AP.m, AcCoA.c, AcCoA.m, OAA.c, OAA.m, Pyr.c, Pyr.m, Cit.c, Cit.m, AKG, SucCoA, Suc, Fum.c, Fum.m, Mal.c, Mal.m, Gln, Glu, Asn, Asp, Ser, Gly, C1, Pro, Val, Ile, Leu, Thr, Phe, Tyr, Met, Lys, His, Arg.

Unbalanced metabolite pools: AO.ext, AP.ext, Ao.snk, Ap.snk, Cit.snk, FA.ext, CO2.ext, Glc.ext, Gal.ext, Lac.ext, Ala.ext, Gln.ext, Glu.ext, Asp.ext, Asn.ext, Ser.ext, Gly.ext, Pro.ext, Val.ext, Ile.ext, Leu.ext, Thr.ext, Phe.ext, Tyr.ext, Met.ext, Lys.ext, His.ext, Arg.ext, Cys.snk, Urea.snk.

**Table S3 - Pearson correlation coefficients between conditions represented in Figure 3.F, respective 95% and 99% confidence intervals (95%CI and 99%CI) and statistical significance.**

	Correlation coefficient	95%CI		99%CI		p-value (two-tailed)
		Lower	Upper	Lower	Upper	
HAV vs LACM&GFAM	0.524	0.503	0.545	0.496	0.551	< 0.001
HAV vs. GFAM d20	0.526	0.505	0.546	0.498	0.553	< 0.001
HAV vs. GLCM d0	0.221	0.193	0.248	0.185	0.257	0.112
HAV vs. GLCM d20	0.238	0.211	0.265	0.202	0.273	0.086
LACM&GFAM vs. GFAM d20	0.987	0.986	0.988	0.986	0.988	< 0.001
LACM&GFAM vs. GLCM d0	0.861	0.853	0.868	0.851	0.87	< 0.001
LACM&GFAM vs. GLCM d20	0.868	0.861	0.875	0.858	0.877	< 0.001
GFAM d20 vs. GLCM d0	0.884	0.878	0.89	0.875	0.892	< 0.001
GFAM d20 vs. GLCM d20	0.88	0.873	0.886	0.871	0.888	< 0.001
GLCM d0 vs. GLCM d20	0.984	0.983	0.985	0.983	0.985	< 0.001

**Table S4 - Euclidean distances between closest neighboring samples represented in PCA plots (Figure 3G and 4A), calculated considering the space defined by the first (PC1) and second (PC2) components.**

	Euclidean distance (Figure 3G)	Euclidean distance (Figure 4A)
HAV vs LACM&GFAM d20	11.55±2.50	81.83±7.92
HAV vs. GFAM d20	11.08±0.94	82.95±3.83
HAV vs. GLCM d0	14.85±2.18	128.04±3.65
HAV vs. GLCM d20	14.34±1.08	82.37±7.35
LACM&GFAM d20 vs. GFAM d20	1.61±0.09	4.38±3.25
LACM&GFAM d20 vs. GLCM d0	8.72±1.04	96.42±0.51
LACM&GFAM d20 vs. GLCM d20	8.19±0.76	29.71±5.49
GFAM d20 vs. GLCM d0	7.94±0.16	93.13±2.66
GFAM d20 vs. GLCM d20	7.24±0.02	26.81±7.66
GLCM d0 vs. GLCM d20	1.32±0.06	67.49±5.63

**Table S5 - Pearson correlation coefficients between conditions represented in Figure 4.B, respective 95% and 99% confidence intervals (95%CI and 99%CI) and statistical significance.**

	Correlation coefficient	95%CI		99%CI		p-value (two-tailed)
		Lower	Upper	Lower	Upper	
HAV vs LACM&GFAM d20	0.885	0.879	0.891	0.877	0.893	< 0.001
HAV vs. GFAM d20	0.878	0.871	0.884	0.869	0.886	< 0.001
HAV vs. GLCM d0	0.763	0.761	0.784	0.757	0.788	< 0.001
HAV vs. GLCM d20	0.840	0.831	0.848	0.829	0.851	< 0.001
LACM&GFAM vs. GFAM d20	0.994	0.994	0.994	0.994	0.994	< 0.001
LACM&GFAM vs. GLCM d0	0.943	0.94	0.946	0.939	0.947	< 0.001
LACM&GFAM vs. GLCM d20	0.957	0.955	0.959	0.954	0.96	< 0.001
GFAM d20 vs. GLCM d0	0.953	0.95	0.956	0.949	0.956	< 0.001
GFAM d20 vs. GLCM d20	0.960	0.958	0.962	0.957	0.963	< 0.001
GLCM d0 vs. GLCM d20	0.965	0.963	0.967	0.962	0.968	< 0.001

**Table S6. Comparison of contractility kinetics and contractile force generated by cells cultivated in LACM&GFAM at d10 and d20.** Data are represented as mean±SD. \*p<0.05; \*\*p<0.01.

	LACM&GFAM d10	LACM&GFAM d20	Statistical Analysis
<b>Force (mM/mm<sup>2</sup>)</b>	0.28±0.10	0.48±0.22	*
<b>% Shortening</b>	5.90±2.17	8.42±3.30	*
<b>Maximum shortening velocity (μm/ms)</b>	0.05±0.02	0.07±0.03	*
<b>Maximum relengthening velocity (μm/ms)</b>	0.03±0.01	0.05±0.02	**